Advances in Science and Technology Research Journal

Advances in Science and Technology Research Journal, 2026, 20(6), 445–456
https://doi.org/10.12913/22998624/218791
ISSN 2299-8624, License CC-BY 4.0

Received: 2026.02.10
Accepted: 2026.04.15
Published: 2026.05.01

Abrasive water jet cutting of composite materials

Xianding Xue[1]

[1] National Technical University of Ukraine "Igor Sikorsky Kyiv Polytechnic Institute", 37, Prospect Beresteiskyi, Kyiv, 03056, Ukraine
E-mail: xiandingx@gmail.com

ABSTRACT

The demand for high-quality surface integrity and precise kerf geometry in composite machining continues to grow, especially in aerospace and automotive industries, making abrasive water jet cutting a key non-thermal machining technology. However, the process involves complex nonlinear and stochastic interactions between the abrasive jet and anisotropic composite materials, which complicate reliable prediction of kerf depth, kerf width, and surface roughness. This work aims to develop a stochastic surface evolution model for abrasive water jet cutting of anisotropic composites, integrating deterministic jet dynamics, material anisotropy, and random particle impact fluctuations. The proposed methodology is based on a stochastic partial differential equation of the Kardar-Parisi-Zhang type, extended with a spatially varying jet intensity distribution and an erosion efficiency function that depends on matrix and fiber hardness, fiber volume fraction, and fiber orientation. The radial distribution of abrasive particle energy is described by a modified Gaussian profile calibrated through Monte Carlo simulations of particle trajectories, accounting for turbulence-induced beam spreading. Numerical simulations are performed on a discretized grid with periodic boundary conditions to reproduce kerf formation and roughness development over time. The results indicate that increasing jet pressure or stand-off distance broadens the energy flux distribution, producing smoother deterministic profiles and slower kerf deepening, while low pressure and short stand-off distance generate narrow, high-intensity jets that promote stronger localized erosion and faster roughness growth. The roughness evolution follows a power-law scaling with growth exponents in the range of 0.60–0.67, indicating kinetic roughening behavior. The proposed model provides a physically consistent tool for predicting kerf geometry and surface integrity and offers practical guidance for optimizing cutting parameters to minimize surface roughness while maintaining machining efficiency.

Keywords: abrasive water jet cutting, anisotropic composites, stochastic surface evolution, Kardar-Parisi-Zhang model, kerf geometry, surface roughness.

INTRODUCTION

Abrasive water jet cutting (AWJC) is a versatile non-traditional machining method for metals, ceramics, and composite materials [1, 2]. It uses a high-velocity water jet with abrasive particles to remove material through micro-erosion. Unlike conventional cutting, AWJC avoids thermal distortion and preserves surface integrity [3, 4]. However, predicting kerf width, penetration depth, and surface roughness remains challenging due to the nonlinear and stochastic nature of jet-material interactions [4].

The behavior of an abrasive water jet is governed by hydrodynamic models coupling liquid, air, and abrasive motion [2, 3]. Jet energy transfer and particle impact velocity are key factors for material removal [1, 3]. For anisotropic composites, heterogeneity and fiber orientation add complexity. Classical erosion theories by Finnie [5] and Bitter [6] describe average material removal rates but cannot capture microstructural roughness. Micro-cutting, cracking, and delamination cause strong spatial variability in erosion and surface morphology. Later models introduced material-specific erosion laws for ceramics and brittle composites [7, 8].

Stochastic surface evolution models, such as the Kardar-Parisi-Zhang (KPZ) framework, account for local diffusion, nonlinearity, and

random perturbations [9]. Hybrid empirical-analytical approaches link kerf characteristics to process parameters such as water pressure, feed rate, abrasive mass flow, and impingement angle [10, 11]. However, regression-based models often ignore stochastic fluctuations affecting final surface morphology [12]. Incorporating anisotropy and stochastic noise allows realistic simulation of 2D cut profiles and surface roughness scaling [13, 14]. Additionally, theoretical studies of stochastic surface growth and kinetic roughening [15, 16] provide a fundamental framework for understanding how deterministic erosion, material heterogeneity, and random fluctuations jointly shape surface morphology. These works demonstrate that surface features evolve self-affinely and can be characterized by universal scaling exponents, offering a solid theoretical basis for applying KPZ-type models to AWJC of composites [17, 18].

Recent studies address AWJC of advanced composites and additively manufactured parts [19, 20]. These works demonstrate the influence of material heterogeneity, jet parameters, and stochastic effects on kerf geometry and surface integrity [21, 22]. Practical challenges in abrasive water jet (AWJ) cutting of carbon fiber-reinforced polymers (CFRP) include minimizing delamination, controlling surface roughness, and optimizing cut quality [23]. These issues are particularly critical in industries like aerospace and automotive, where high-quality CFRP parts are essential [22]. Delamination during the initial piercing stage can compromise the integrity of the material, leading to costly rework [21]. A scientometric analysis has shown significant global interest in the issues of abrasive waterjet machining, highlighting the growing body of research and contributions from countries around the world [24]. Some study addresses these challenges by using an artificial neural network (ANN) to optimize process parameters and enhance the performance of AWJ piercing in CFRP materials [25,26]. Nevertheless, integrated models combining deterministic hydrodynamics, stochastic particle impacts, and anisotropic composite responses remain limited [27].

Unlike existing empirical, regression-based, or purely hydrodynamic approaches, the present study introduces a physically grounded stochastic surface evolution framework that explicitly couples deterministic jet intensity distribution, anisotropic composite response, and noise-driven particle impact fluctuations within a unified continuum model.

The innovation of this work lies in extending a KPZ-type stochastic partial differential equation to abrasive water jet cutting by incorporating:

- a turbulence-corrected spatial energy distribution of the jet;
- (an anisotropy-dependent erosion efficiency function linked to fiber orientation and volume fraction;
- (a scaling analysis of surface roughness evolution under realistic cutting conditions.

This integrated formulation enables simultaneous prediction of kerf geometry and kinetic roughening behavior, which has not been systematically addressed in previous AWJC modeling studies.

The aim of this study is to develop a stochastic surface dynamics model for AWJC of anisotropic composites. The model integrates hydrodynamic jet parameters, empirical erosion efficiency, and anisotropic material responses, while accounting for stochastic particle impacts. This framework enables simulation of realistic cut surfaces, evaluation of roughness parameters, and analysis of scaling relations between surface morphology, material properties, and process variables. The approach provides a physically consistent tool to improve cut precision, process efficiency, and surface integrity in machining advanced composites.

MATERIALS AND METHODS

Materials

Material properties were selected based on typical values reported for polymer-matrix composites commonly processed by abrasive water jet cutting. The composite is treated as a system comprising a relatively compliant matrix reinforced with high-hardness fibers, which leads to pronounced mechanical anisotropy. Understanding this structural heterogeneity is essential for explaining its interaction with the abrasive jet. In particular, the contrast in mechanical behavior between the constituents governs how impact energy is absorbed, redistributed, and ultimately transformed into material removal.

The material removal in AWJC of fiber-reinforced composites is governed by the energy transfer from high-velocity abrasive particles to the heterogeneous composite surface. The local erosion rate depends on jet pressure, particle velocity, fiber orientation, and the hardness contrast between matrix and reinforcement. The local

material removal rate $A(\vartheta)$, which represents the instantaneous velocity of material removal (m/s) at a surface point characterized by the fiber orientation angle ϑ, can be expressed as

$$A(\vartheta) = C_A \frac{K(\vartheta) E_p}{H_{eff}(\vartheta)} \tag{1}$$

where: C_A is a dimensional scaling constant with $[C_A] = m^{-2}s^{-1}$, E_p is the average kinetic energy of an impacting abrasive particle (J), $H_{eff}(\vartheta)$ is the effective hardness (Pa) that characterizes the local resistance of the composite, and $K(\vartheta)$ is a dimensionless efficiency factor describing the influence of fiber orientation and volume fraction.

The parameter C_A incorporates both the particle impact frequency (number of particles per unit area per second) and the effective fraction of energy contributing to material removal, thereby connecting the microscopic particle-scale physics to the measurable macroscopic erosion rate. The effective hardness of the composite appearing in Equation 1 is given by

$$H_{eff}(\vartheta) = H_m(1 - V_f) + \\ + H_f V_f \cos^2 \vartheta \tag{2}$$

where: H_m and H_f are the hardnesses of the matrix and fibers, respectively, and V_f is the fiber volume fraction.

The $\cos^2 \vartheta$ term accounts for the mechanical anisotropy – fibers oriented perpendicular to the jet ($\vartheta = 0$) resist erosion more effectively, while fibers aligned parallel to the surface contribute less to local hardness. This expression is consistent with empirical models for composite erosion resistance reported in [4, 8].

The mean particle energy E_p is assumed to be proportional to the jet pressure P, following the analysis of Hashish [1] and Momber and Kovacevic [2]:

$$E_p = c_E P \tag{3}$$

where: c_E is the energy–volume coefficient ($[c_E] = m^3$).

It represents the effective interaction volume of the jet with the target, or equivalently, the portion of the pressurized fluid energy transferred to each abrasive particle. The exact value of c_E depends on particle size, density, velocity, and jet parameters such as standoff distance and nozzle geometry.

The anisotropic efficiency factor $K(\vartheta)$ appearing in Equation 1 accounts for the reduction in erosion efficiency with increasing fiber content and misalignment:

$$K(\vartheta) = \frac{\cos \vartheta}{1 + \alpha V_f} \tag{4}$$

where: α is a dimensionless empirical constant that characterizes the interaction between the jet and the reinforcing fibers.

Larger α values indicate stronger shielding effects of fibers, leading to reduced removal efficiency for composites with high fiber fractions.

Substituting Equation 2–4 into Equation 1 yields a more explicit expression for the local material removal rate in composites:

$$A(\vartheta) = C_A \frac{K(\vartheta) c_E P}{H_m(1 - V_f) + \\ + H_f V_f \cos^2 \vartheta} \tag{5}$$

This predicts that the erosion velocity increases linearly with jet pressure and decreases with composite hardness or fiber volume fraction. The dependence on fiber orientation is strongly anisotropic, with the highest removal rate when fibers are perpendicular to the jet and the lowest when they are parallel to the surface.

Thus, the proposed formulation establishes a direct relationship between the governing material properties, structural anisotropy, and process parameters, providing a physically interpretable framework for predicting local material removal. To assess the validity and applicability of this model, its predictions must be compared with experimentally measured erosion characteristics under controlled processing conditions.

Characteristic experimental parameters

In practical studies of AWJ machining and erosion of composites, several key parameters are measured to validate and calibrate such models. The jet pressure P is usually varied in the range of 100–400 MPa, directly controlling the kinetic energy of particles and thus the erosion intensity [1, 2]. The abrasive mass flow rate dm_a / dt (typically 50–300 g/min) and particle size d_p (commonly 50–150 μm) determine the total number of impacts per unit time and the effective area of energy transfer. These quantities influence

the scaling constant C_A, which is experimentally identified by correlating measured erosion depths with process parameters.

The stand-off distance between the nozzle and the target surface was set in the range of 1–10 mm for the present study. This parameter affects jet divergence and particle deceleration, with smaller distances increasing both the impact velocity and energy concentration, while larger distances reduce removal efficiency due to jet spreading and particle energy loss, consistent with experimental observations [2, 7].

Material properties were chosen based on typical values reported for polymer-matrix composites. The matrix hardness H_m ranges from 0.1 to 1 GPa, and the fiber hardness H_f can reach 10–20 GPa for carbon or glass fibers, as determined from microindentation tests [4, 10]. The fiber volume fraction V_f was selected between 0.3 and 0.6, reflecting structural composites and controlling the effective hardness $H_{eff}(\vartheta)$ and anisotropy of erosion.

Experimentally, the cutting rate or erosion depth is determined by profilometry or microscopy after fixed exposure times. The resulting data are fitted to the analytical expression for $A(\vartheta)$ to extract empirical parameters such as C_A, c_E, and α.

To validate and calibrate the surface evolution and material removal models, key process parameters were selected based on typical AWJC experiments and literature data [1,2,7,10]. These parameters govern the kinetic energy of abrasive particles, the interaction between the jet and composite surface, and the resulting kerf geometry and surface roughness.

These parameters can be conveniently summarized in a Table 1.

Experimentally, erosion depth and surface roughness are measured via profilometry or microscopy after fixed exposure times, enabling calibration of the model against observed kerf profiles [11,12]. The combination of these parameters determines the scaling constants in the model, the effective erosion rates, and the stochastic surface roughness evolution [1,2,4,8].

Surface evolution model for AWJ cutting process

The AWJ cutting process is represented through the temporal evolution of a surface height function $h(x, y, t)$, which characterizes the local kerf depth produced by particle-induced erosion. Here, x and y denote the in-plane coordinates within the jet-impact region, and t is time. The surface evolution is governed by a nonlinear stochastic partial differential equation that incorporates erosion, smoothing, and noise-driven roughness. To account for AWJ-specific effects such as the spatial distribution of abrasive energy, an additional term describing jet-material interaction is introduced. The governing evolution equation is given by

$$\frac{\partial h}{\partial t} = A(x,y)I(x,y) + \nu\nabla^2 h + \\ + \frac{\lambda}{2}(\nabla h)^2 + \xi(x,y,t) \tag{6}$$

where: $A(x, y)$ is given by Equation 5, $I(x, y)$ is the normalized jet intensity distribution, ν is a smoothing coefficient accounting for surface diffusion and redistribution of removed material, λ slope-dependent erosion, and $\xi(x,y,t)$ is a stochastic noise term describing the random arrival and energy dispersion of abrasive particles.

The first term on the right-hand side of Equation 6, $A(x, y)$ $I(x, y)$, represents the deterministic erosion rate, describing local material removal according to the jet's radial intensity profile $I(x, y)$. High-intensity regions erode faster, forming deeper kerfs, while peripheral areas erode slower, producing tapered surfaces [15]. The Laplacian term $\nu\nabla^2 h$ provides a stabilizing effect, counteracting excessive roughness growth by promoting diffusion-like smoothing of the surface. The nonlinear gradient term $(\nabla h)^2$ accounts for the anisotropic dependence of erosion on the local surface slope, reflecting that oblique impacts remove less material than normal ones. The stochastic term $\xi(x,y,t)$ represents random fluctuations in particle impacts, including variations in trajectories, sizes, and impact frequency, and is modeled as Gaussian white noise.

Together, these terms allow the model to capture both the macroscopic kerf profile and the microscopic roughness evolution, providing a unified framework for predicting surface morphology under different jet and material conditions. Surface evolution is governed solely by local jet interactions and intrinsic material properties, enabling physically consistent simulations of kerf formation and roughness development.

Table 1. Experimental parameters

Parameter	Symbol	Range / Value	Notes
Jet pressure [1,2].	P	100–400 MPa	Controls particle kinetic energy
Abrasive flow rate	dm_a/dt	50–300 g/min	Number of particles impacting surface
Particle size [2,7]	d_p	50–150 μm	Influences local erosion
Stand-off distance	SOD	1–10 mm	Affects jet spreading and impact velocity
Matrix hardness	H_m	0.1–1 GPa	Polymer matrix resistance
Fiber hardness	H_f	10–20 GPa	Carbon or glass fibers
Fiber volume fraction	V_f	0.3–0.6	Controls effective hardness and anisotropy

Radial distribution of abrasive particles in water jets

A key factor in AWJ machining is the radial distribution of abrasive particles within the water jet, which appears in Equation 6 and governs local material removal as well as the resulting kerf profile. Particle concentration and energy flux are nonuniform across the jet radius, typically peaking near the axis and decaying toward the periphery [2,3]. This behavior can be modeled using a normalized radial intensity distribution:

$$I(r) = I_0 \exp\left[-\left(\frac{r}{\sigma}\right)^n\right] \tag{7}$$

where: r is the radial distance from the jet centerline, I_0 is the peak intensity, σ_b is effective radial spread, and n is an exponent controlling the sharpness of the profile.

Values of n between 1.5 and 2.5 are typical for AWJs [2]. This distribution is incorporated into the KPZ-based surface evolution model through the erosion term, enabling spatially resolved prediction of kerf depth and surface roughness.

For many practical cases, despite turbulence, the particle energy flux can be approximated by a Gaussian profile:

$$I(r) = \frac{I_0}{\sqrt{2\pi}\sigma(t)} \exp\left[-\frac{r^2}{2\sigma^2(t)}\right] \tag{8}$$

where: $\sigma(t) = \sqrt{\sigma_0^2 + 2D_t t_f}$, with σ_0 being is the characteristic nozzle radius, D_t the turbulent diffusion coefficient, and t_f the particle flight time.

Experiments show that the jet core expands downstream, and σ increases approximately with the square root of the stand-off distance, supporting the Gaussian approximation [1, 2].

The radial distribution of particle flux defines the spatial pattern of erosive energy delivered to the surface, which is linked to local material removal rates through the AWJ material removal model. This relationship is critical for simulating anisotropic erosion and optimizing cutting conditions, including nozzle geometry, feed rate, and jet pressure.

RESULTS AND DISCUSSION

The AWJC process is modeled through computer simulations based on solving governing equations that describe material removal. First, the radial distribution of abrasive particles in the jet is analyzed to determine how particle concentration and velocity vary across the jet, yielding the normalized intensity function $I(r)$. Then, this information is used in the surface evolution model, which numerically solves Equation 6 for the cutting depth $h(x, y, t)$, accounting for jet incidence angle, fiber orientation, and material anisotropy. This computational approach enables prediction of local erosion rates and surface roughness, linking the jet parameters and material properties to the resulting surface quality.

In this study, the surface roughness of the cut specimens is represented using parameters derived from experimental profilometric measurements (e.g., [11, 12]). The surface height was discretized into N sampling points along a selected profile, and the roughness metrics were calculated as

$$R_a = \frac{1}{N}\sum_{i=1}^{N} |h_i - \bar{h}|$$
$$R_q = \sqrt{\frac{1}{N}\sum_{i=1}^{N}(h_i - \bar{h})^2} \tag{9}$$

where: h_i denotes the measured height at the i-th point and $\overline{h}$ is the mean surface level within the sampling length.

\The parameter R_a represents the mean amplitude of local asperities, whereas R_q provides a statistically weighted measure that is more sensitive to sharp peaks and deep valleys. These parameters were used to calibrate the model, reproducing both the mean erosion rate and the multi-scale evolution of surface morphology under AWJ cutting.

Simulation of abrasive particle distribution in water jets

The simulations were carried out to investigate how the radial distribution of particle energy flux $I(r)$ in an abrasive jet depends on turbulence, nozzle pressure, and stand-off distance. The resulting intensity field represents the spatial structure of the deterministic source term in the rate expression $A(\vartheta)I(r)$ of Eq. (6), which governs the mean surface height evolution in a KPZ-type continuum framework. To quantify the influence of turbulence near the nozzle exit, a preliminary Monte Carlo simulation was performed to generate the distribution of particle impacts in the cross-section of a jet. Particle coordinates (x, y) were sampled from a normal distribution with a standard deviation σ_0, representing the characteristic initial radius of the jet. The maximum radial distance of generated particles was limited to R = $4\sigma_0$ capturing the majority of the beam while maintaining clear visualization. The resulting radial density profile $I_{MC}(r)$ from the Monte Carlo simulation was compared with the modified Gaussian approximation (see Equation 8), which is subsequently adjusted as $I_0 \rightarrow I_0(1+\alpha r / R)$. As shown in Figure 1, the Monte Carlo data show almost complete agreement with the modified Gaussian curve, taking into account the correction factor $\alpha = 0.3$. This correction reproduces the enhanced peripheral intensity observed in the stochastic simulation and captures the asymmetric influence of turbulent eddies on particle flux near the nozzle exit.

To explore how process conditions modify this distribution, additional simulations were performed using base parameters $\sigma_0 = 0.8 \cdot 10^{-3}$ m, $I_0 = 1.0$, $\alpha = 0.3$, R = $3.2mm$, $t_{f0} = 10$ ms, and $D_{t0} = 0.5$ mm^2 / ms. The modeling was first conducted to study the effect of nozzle pressure, varied between 150 and 250 MPa, on the beam profile. The turbulent diffusion coefficient was assumed to scale approximately linearly with pressure according to $D_t(P) = D_{t0}P / 200$. As the pressure rises, turbulence intensifies, leading to larger values of σ_b and thus a broader intensity profile. The results in Figure 2 show that at 150 MPa the distribution is narrow and sharply peaked at the center, while at 250 MPa it becomes flatter, with energy spread across a wider region. Physically, higher pressure yields a more uniform but less localized surface modification rate, as the product $A(\vartheta)I(r)$ becomes spatially smoother

The next set of simulations focused on the influence of stand-off distance L_s, modeled by scaling the particle flight time as $t_f(L_s) = t_{f0}L_s / 10$

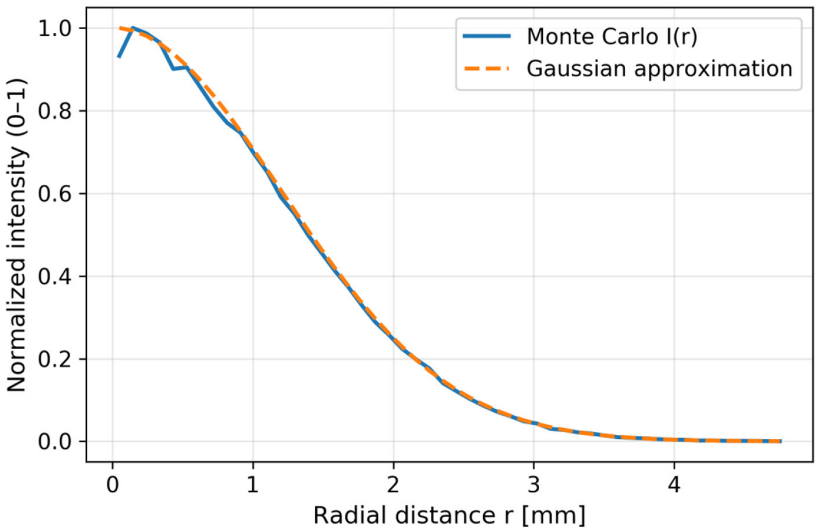

Figure 1. Monte Carlo simulation of the radial distribution of abrasive particles compared with a modified Gaussian approximation

. Calculations for L_s = 10, 20, and 30 mm demonstrate that increasing the stand-off distance increases beam broadening, since particles have more time to diffuse laterally before impact. As presented in Figure 3, at L_s = 10 mm the jet remains tightly focused and produces a concentrated intensity peak, while at L_s = 30 mm the intensity profile becomes wider with a lower maximum value. This trend indicates that greater stand-off distances lead to reduced peak growth rates and more diffuse deposition patterns, consistent with the idea that the incoming flux acts as a spatially distributed source of surface evolution.

Both parameter studies show that increasing either nozzle pressure or stand-off distance enhances turbulent diffusion and broadens the energy distribution. In the framework of surface growth, these effects correspond to a smoother and less localized deterministic source term in Equation 6. Specifically, low-pressure and short stand-off conditions produce narrow, high-intensity profiles that concentrate the growth source in a small area, promoting stronger local height increase and nonlinear roughening. Conversely, high-pressure or long stand-off configurations generate broader, lower-intensity distributions, leading to more spatially uniform deposition and slower local growth. This interpretation highlights how operating parameters can be directly linked to the spatial structure of the deterministic source term driving KPZ-type surface evolution.

The results thus demonstrate that turbulent spreading of abrasive or energetic particles has a decisive effect on the shape of $I(r)$ and must be incorporated into any realistic model of deterministic surface evolution. The inclusion of the turbulence correction factor $\alpha = 0.3$, derived from Monte Carlo analysis, enables the analytical profile to capture these effects accurately. Together, the presented simulations provide a physically consistent description of how jet operating conditions modulate the spatial structure of the energy flux that drives the KPZ-type surface evolution described by Equation 6.

Cutting depth and surface roughness dynamics

In numerical models of AWJC of composite materials, the deterministic intensity field $I(r)$ is considered the main driving factor for surface erosion. This deterministic component is complemented by stochastic fluctuations in the spirit of KPZ-type dynamics, allowing analysis of both the macroprofile of the kerf and the microscale roughness developing over time.

The model composite Equation 5 consists of a soft matrix with hardness H_m = 2 GPa and stiff reinforcing fibers with hardness H_f = 10 GPa, occupying a volume fraction V_f = 0.3, which corresponds to CFRP, GFRP, and metal-matrix composites frequently processed by AWJC. The fiber orientation angle $\vartheta = 30^0$ is chosen to represent an off-axis reinforcement typical of layered composites. From these parameters, the effective hardness H_{eff} and angular correction $K(\vartheta)$, Equation 4, yield an erosion coefficient A ≈ 2 · 10^{-2} mm/s at a jet pressure P = 200 MPa, with C_A = 10^{-6} and C_E = 10^{-2}.

Simulations were performed on a 60-by-60 node grid with periodic boundary conditions, time step 0.01 s, and total simulation time 10 s.

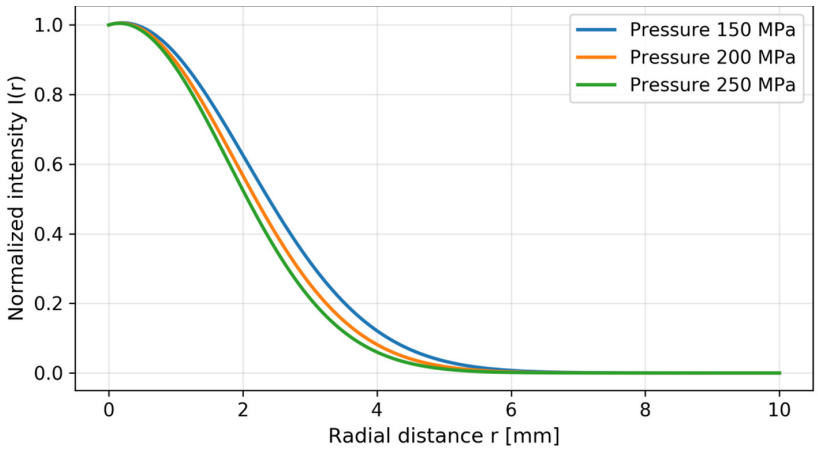

Figure 2. Effect of nozzle pressure on the normalized radial intensity profile. Increasing pressure broadens the distribution and reduces the peak intensity

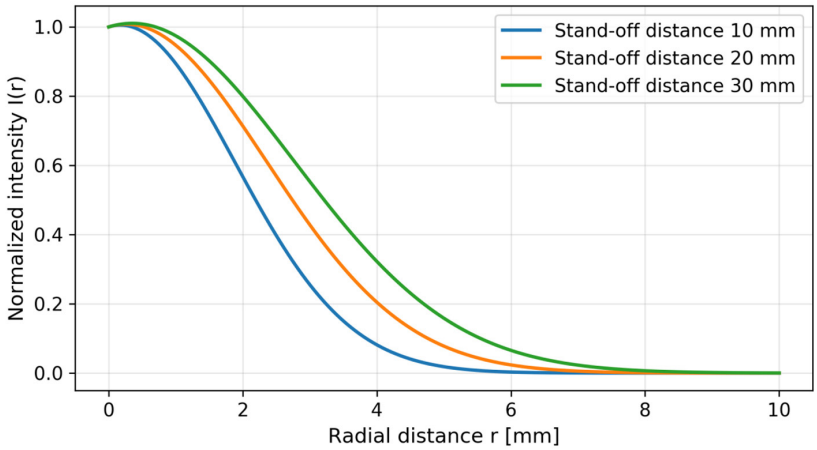

Figure 3. Effect of stand-off distance on the normalized intensity profile

The intensity field follows a normalized Gaussian distribution Equation 8 with the maximum at the jet center scaled to unity.

At early stages, the surface forms a smooth paraboloid kerf under the influence of the deterministic erosion flux. Stochastic fluctuations at this stage are negligible. As time progresses, small random deviations are amplified by nonlinear terms $(\nabla h)^2$, leading to the development of microscale peaks and valleys, characteristic of kinetic surface roughening.

Figure 4 shows the evolution of cross-sectional kerf profiles along the jet axis from t=0 to t=10 s. The central region continuously deepens while the lateral slopes widen, reflecting the growth of the effective erosion zone. At later stages, microscale asperities and depressions appear due to the accumulation of stochastic fluctuations.

The temporal evolution of the roughness extracted from the numerical simulations reveals a systematic increase in both $R_a(t)$ and $R_q(t)$, Equation 9, with no indication of saturation. The behavior observed in Figure 5 is characteristic of kinetic roughening: the roughness grows monotonically while maintaining an approximately linear trend on a log–log scale. Such scaling behavior suggests that the growth process is governed by self-affine dynamics, in which roughness follows a power-law dependence on time.

To quantify this trend, the roughness growth is approximated by a general power-law function, $R(t) = At^{\beta}$. Fitting the numerical data yields $R_a(t) = A_a t^{\beta_a}$ and $R_q(t) = A_q t^{\beta_q}$, where $\beta_a \approx 0.617$ and $\beta_q \approx 0.666$, and prefactors $A_a \approx 0.34034$ and $A_q \approx 0.41462$. The fitted curves in Figure 5 closely follow the numerical roughness data over the entire time interval, confirming the validity of the power-law description. The larger growth exponent for $R_q(t)$ indicates that extreme height fluctuations grow faster than the mean absolute deviation, reflecting the nonlinear nature of stochastic surface evolution. These results demonstrate continuous roughness growth within the kinetic roughening regime, with the correlation length remaining smaller than the system size. The logarithmic dependence in Figure 6 confirms the linear trend on a log-log scale, demonstrating the validity of the power-law approximation and the scaling nature of stochastic roughening. These results provide a comprehensive understanding of both deterministic and stochastic contributions to kerf formation and surface roughening. They emphasize how variations in material properties, fiber orientation, and abrasive jet parameters quantitatively influence the local erosion rates and kerf geometry. By linking theoretical predictions with experimentally measurable quantities such as erosion depth, kerf width, and surface roughness, this analysis establishes a solid foundation for interpreting the mechanisms of material removal and assessing their practical implications in optimizing AWJ machining processes and improving surface quality control.

The proposed stochastic KPZ-type model provides an effective framework for describing the abrasive water jet cutting process in anisotropic composites. While most studies on abrasive water jet cutting focus on empirical correlations between process parameters and kerf characteristics, the present work integrates

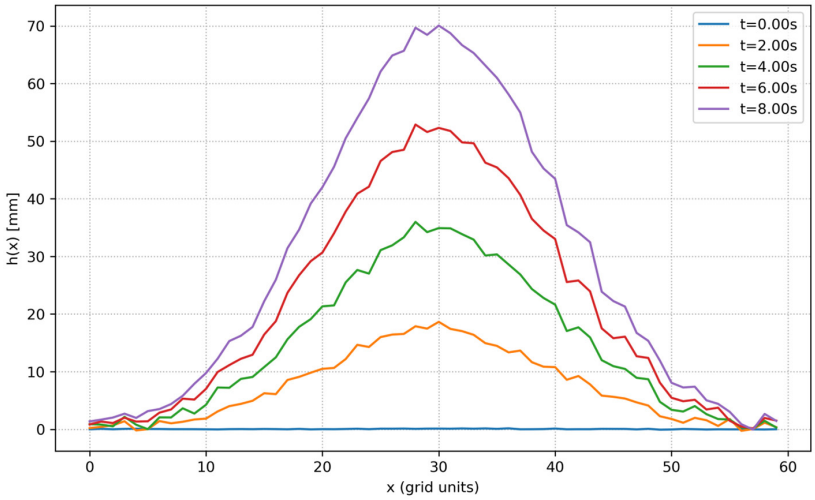

Figure 4. Temporal evolution of cross-sectional profiles along a plane passing through the jet axis

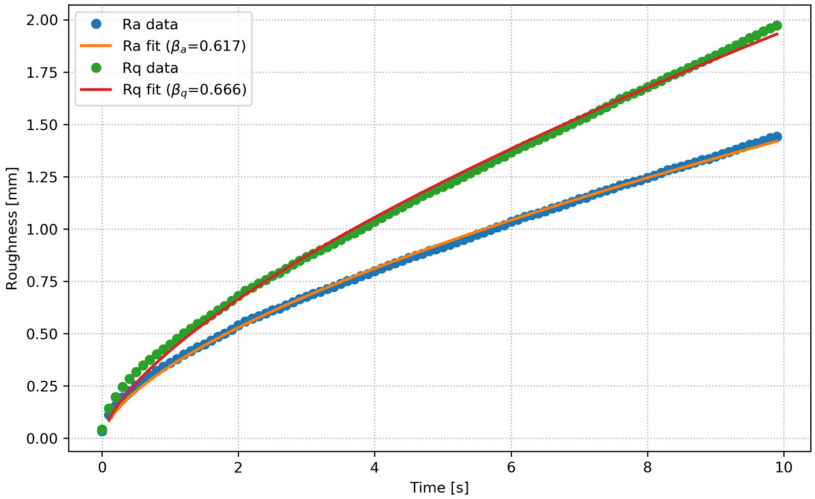

Figure 5. Surface roughness evolution with corresponding power-law fits

deterministic jet intensity distribution with stochastic surface evolution, enabling simultaneous prediction of macroscopic kerf geometry and microscopic roughness dynamics. This approach bridges classical erosion theories and modern stochastic surface growth concepts, providing a unified description of how jet parameters and material anisotropy influence both depth and surface morphology.

The radial distribution of abrasive particles plays a central role in determining kerf geometry. The Monte Carlo-based analysis of particle trajectories reveals that turbulence at the nozzle exit broadens the energy flux distribution beyond a simple Gaussian profile, particularly at larger radii. This finding is consistent with experimental observations of jet spreading and enhanced peripheral erosion, and it highlights the importance of incorporating turbulence-corrected intensity profiles in realistic AWJ models. Increasing nozzle pressure and stand-off distance both intensify turbulent diffusion, leading to broader intensity profiles and smoother deterministic source terms. As a consequence, higher pressure or larger stand-off distances reduce the localization of erosion, producing shallower but wider kerfs. These effects explain why, in practice, cutting under moderate pressure and short stand-off distances provides a balance between penetration and surface quality.

A key outcome of the simulations is the power-law growth of surface roughness, with estimated scaling exponents of 0.617 for the mean absolute deviation and 0.666 for the root mean square deviation. These values indicate that surface roughness increases rapidly during the cutting process and does not reach saturation within the simulated

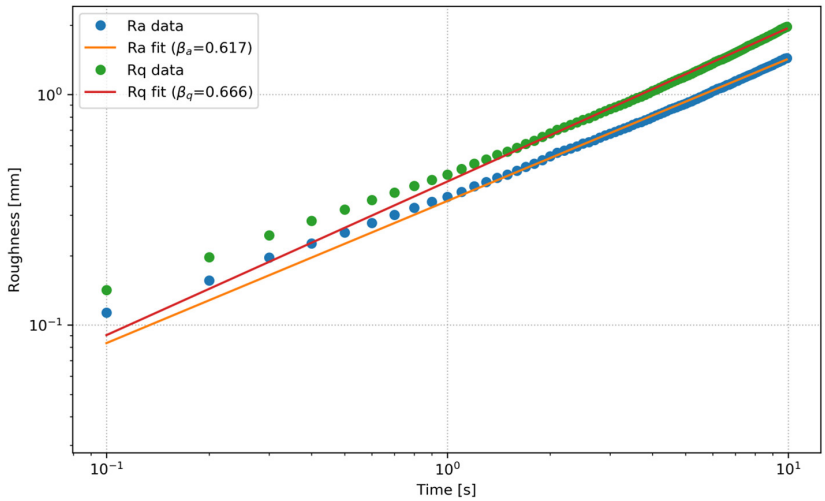

Figure 6. Log-log plot of $R_a(t)$ and $R_q(t)$ with fitted lines, confirming the power-law scaling characteristic of stochastic roughening

time interval. The difference between the two exponents suggests that extreme height deviations (peaks and valleys) develop faster than the average asperity amplitude, which is consistent with the nonlinear amplification of stochastic perturbations in KPZ-type dynamics. Such high growth exponents imply that even small stochastic fluctuations can lead to significant roughness evolution, underscoring the importance of noise effects in composite machining. The obtained exponents also suggest that AWJ erosion of anisotropic composites may belong to a distinct class of correlated growth processes, influenced by material heterogeneity and turbulence-modified forcing.

A limitation of the present model is that it is based on a two-dimensional surface evolution equation and assumes a homogeneous statistical distribution of material properties within the computational domain. The model does not explicitly account for delamination, fiber pull-out, or matrix cracking mechanisms that can occur in layered composites, nor does it include detailed coupling between hydrodynamic jet behavior and particle-surface interactions beyond the simplified intensity profile. The stochastic noise is represented as Gaussian white noise, which may not fully capture correlated fluctuations arising from particle clustering or jet instabilities. Consequently, the quantitative predictions should be interpreted as qualitative trends and require experimental validation for specific composite systems and cutting conditions.

Anisotropic material properties strongly affect erosion efficiency and kerf shape. Higher fiber volume fractions and fiber orientations perpendicular to the jet increase local hardness and reduce material removal rate, resulting in more pronounced kerf tapering and surface irregularities. These observations are important for machining carbon and glass fiber composites, where delamination and surface damage critically depend on local erosion dynamics. The model shows that the deterministic intensity field governs the macroscopic kerf profile, while stochastic fluctuations determine the kinetic roughening behavior, linking operating parameters directly to surface integrity.

Overall, the study demonstrates that the interplay between deterministic jet forcing, anisotropic material response, and stochastic particle impacts governs both kerf formation and roughness evolution. The model offers a physically consistent tool for predicting surface morphology and for optimizing AWJ parameters to achieve improved cut quality. The framework may be further refined by incorporating experimental profilometry data, more advanced noise models, and three-dimensional surface evolution, which could enhance its predictive capability and practical applicability.

CONCLUSIONS

This study demonstrates that a stochastic KPZ-type surface evolution model, combined with a realistic representation of abrasive jet intensity distribution, provides a comprehensive framework for analyzing abrasive water jet cutting of anisotropic

composite materials. The integration of deterministic jet forcing, anisotropic material response, and stochastic particle impacts allows simultaneous prediction of kerf geometry and surface roughness evolution, which is essential for improving cut quality in composite machining. The Monte Carlo analysis of particle distribution confirms that turbulence at the nozzle exit broadens the energy flux profile, producing a more uniform but less localized erosion source and highlighting the importance of incorporating turbulence effects in modeling. Numerical simulations show that surface roughness grows according to a power-law with scaling exponents of 0.617 and 0.666, indicating rapid kinetic roughening and the dominant role of stochastic fluctuations in the development of microscale asperities. The results also indicate that higher jet pressure and larger stand-off distance broaden the intensity profile, reducing local growth rates and smoothing the kerf profile, while higher fiber volume fraction and unfavorable fiber orientation increase effective hardness and promote surface irregularities. Based on these findings, practical recommendations for AWJ cutting of composites include using moderate pressures (150-200 MPa) to balance penetration and surface stability, maintaining short stand-off distances (5-10 mm) to limit beam spreading and preserve kerf localization, and orienting fibers closer to the cutting direction to reduce anisotropic shielding effects. The proposed model thus offers a physically consistent tool for predicting cutting outcomes and supports further development of stochastic erosion modeling for advanced composites.

REFERENCES

1. Hashish M. A modeling study of metal cutting with abrasive waterjets. J. Eng. Mater. Technol. 1984; 106: 88–100. https://doi.org/10.1115/1.3225682
2. Momber A.W., Kovacevic R. Principles of abrasive water jet machining. London: Springer; 1998. https://doi.org/10.1007/978-1-4471-1572-4
3. Akkurt A., Külekci M.K., Seker U., Ercan F. Effect of feed rate on surface roughness in abrasive waterjet cutting applications. J. Mater. Process. Technol. 2004; 147: 389–396. https://doi.org/10.1016/j.jmatprotec.2004.01.013
4. Du M., Zhong W., Song Z., Teng J., Liang W., Wang H. Advanced waterjet technology for machining beveled structures of high-strength and thick material. Machines. 2024; 12(6): 408. https://doi.org/10.3390/machines12060408
5. Finnie I. Erosion of surfaces by solid particles. Wear. 1960; 3: 87–103. https://doi.org/10.1016/0043-1648(60)90055-7
6. Bitter J.G.A. A study of erosion phenomena: Part II. Wear. 1963; 6: 5–21, 169–190. https://doi.org/10.1016/0043-1648(63)90073-5
7. Zhu H.T., Huang C.Z., Wang J., Zhao G.Q., Li Q.L. Modeling material removal in fracture erosion for brittle materials by abrasive waterjet. Adv. Mater. Res. 2009; 76–78: 357–362. https://doi.org/10.4028/www.scientific.net/AMR.76-78.357
8. Hlaváč L.M., Štefek A., Tyč M., Krajcarz D. Influence of material structure on forces measured during abrasive waterjet (AWJ) machining. Materials. 2020; 13(17): 3878. https://doi.org/10.3390/ma13173878
9. Kardar M., Parisi G., Zhang Y.C. Dynamic scaling of growing interfaces. Phys Rev Lett. 1986; 56: 889–892. https://doi.org/10.1103/PhysRevLett.56.889
10. Alberdi A., Rivero A., Carrascal A., Lamikiz A. Kerf profile modelling in Abrasive Waterjet milling. Mater Sci Forum. 2012; 713: 91–96. https://doi.org/10.4028/www.scientific.net/MSF.713.91
11. Hlaváč L.M. Revised model of abrasive water jet cutting for industrial use. Materials (Basel). 2021; 14: 4032. https://doi.org/10.3390/ma14144032
12. Płodzień M., Żyłka Ł., Żak K., Wojciechowski S. Modelling the kerf angle, roughness and waviness of the surface of Inconel 718 in an abrasive water jet cutting process. Materials (Basel). 2023; 16(15): 5288. https://doi.org/10.3390/ma16155288
13. Barabási A.L., Stanley H.E. Fractal concepts in surface growth. Cambridge: Cambridge University Press; 1995.
14. Kumaran S.T., Ko T.J., Uthayakumar M., Islam M.M. Prediction of surface roughness in abrasive water jet machining of CFRP composites using regression analysis. J Alloys Compd. 2017; 724: 1037–1045. https://doi.org/10.1016/j.jallcom.2017.07.108
15. Makeev M.A., Cuerno R., Barabási A.L. Morphology of ion-sputtered surfaces. Nucl Instrum Methods Phys Res B. 2002; 197: 185–227. https://doi.org/10.1016/S0168-583X(02)01436-2
16. Krim J., Palasantzas G. Experimental observations of self-affine scaling and kinetic roughening at sub-micron lengthscales. Int J Mod Phys B. 1995; 9(6): 599–632. https://doi.org/10.1142/S0217979295000239
17. Cuerno R., Barabási A.L. Dynamic scaling of ion-sputtered surfaces. Phys Rev Lett. 1995; 74: 4746–4749. https://doi.org/10.1103/PhysRevLett.74.4746
18. Rost M., Krug J. Coarsening of surface structures in unstable epitaxial growth. Phys Rev E. 1997; 55(4): 3952–3957. https://doi.org/10.1103/PhysRevE.55.3952
19. Xue X., Salenko O., Habuzian H., Havrushkevych A. A review of abrasive water jet cutting

technology for composite materials. Mechan Adv Technol. 2025; 9(3): 372–385. https://doi.org/10.20535/2521-1943.2025.9.3(106).315941

20. Hussien A.A., Qasem I., Kataraki P.S., Al-Kouz W.G., Janvekar A.A. Studying the performance of cutting carbon fibre-reinforced plastic using an abrasive water jet technique. Strojniški vestnik – Journal of Mechanical Engineering. 2021; 67(4): 125–141. https://doi.org/10.5545/sv-jme.2021.7141
21. Shekar A.C., Sawalmeh A., Zitoune R., Hof L.A. Optimization of surface texturing parameters in additively manufactured continuous fiber composites using abrasive waterjet technique for composite repair applications. Compos Part A Appl Sci Manuf. 2025; 190: 108698. https://doi.org/10.1016/j.compositesa.2024.108698
22. Ergene B., Bolat Ç. A review on the recent investigation trends in abrasive waterjet cutting and turning of hybrid composites. Sigma J Eng Nat Sci. 2019; 37(3): 989–1016.
23. Rowe A., Pramanik A., Basak A.K., Prakash C., Subramaniam S., Dixit A.R., Radhika N. Effects of Abrasive Waterjet Machining on the Quality of the Surface Generated on a Carbon Fibre Reinforced Polymer Composite. Machines. 2023; 11(7): 749. https://doi.org/10.3390/machines11070749
24. Lusi N., Catrawedarma I.G.N.B., Gebremariam M., Saptaji K., Azhari A. A four-decade of abrasive waterjet processing technology (1980-2023): a scientometric analysis. Manuf Rev. 2025; 12: 15. https://doi.org/10.1051/mfreview/2025011
25. Khudhir W.S., Abbood M.Q., Shukur J.J. Multi-criteria decision making of abrasive water jet machining process for 2024-T3 alloy using hybrid approach. Adv Sci Technol Res J. 2022; 16(5): 155–162. https://doi.org/10.12913/22998624/154040
26. Popan I.A., Bocăneț V.I., Softic S., Popan A.I., Panc N., Balc N. Artificial intelligence model used for optimizing abrasive water jet machining parameters to minimize delamination in carbon fiber-reinforced polymer. Appl Sci. 2024; 14(18): 8512. https://doi.org/10.3390/app14188512
27. Zou X., Fu L., Wu L., Zuo W. Research on multiphase flow and nozzle wear in a high-pressure abrasive water jet cutting head. Machines. 2023; 11(6): 614. https://doi.org/10.3390/machines11060614